

# Measurement of the $B \rightarrow D\ell\nu$ Branching Fractions and Form Factor

CLEO Collaboration

(August 22, 2018)

## Abstract

Using a sample of  $3.3 \times 10^6$   $B$ -meson decays collected with the CLEO detector at the Cornell Electron Storage Ring, we have studied  $B^- \rightarrow D^0\ell^-\bar{\nu}$  and  $\bar{B}^0 \rightarrow D^+\ell^-\bar{\nu}$  decays, where  $\ell^-$  can be either  $e^-$  or  $\mu^-$ . We distinguish  $B \rightarrow D\ell\nu$  from other  $B$  semileptonic decays by examining the net momentum and energy of the particles recoiling against  $D - \ell$  pairs. We find  $\Gamma(B \rightarrow D\ell\nu) = (14.1 \pm 1.0 \pm 1.2) \text{ ns}^{-1}$  and derive branching fractions for  $B^- \rightarrow D^0\ell^-\bar{\nu}$  and  $\bar{B}^0 \rightarrow D^+\ell^-\bar{\nu}$  of  $(2.32 \pm 0.17 \pm 0.20)\%$  and  $(2.20 \pm 0.16 \pm 0.19)\%$  respectively, where the uncertainties are statistical and systematic. We also investigate the  $B \rightarrow D\ell\nu$  form factor and the implication of the result for  $|V_{cb}|$ .

J. Bartelt,<sup>1</sup> S. E. Csorna,<sup>1</sup> K. W. McLean,<sup>1</sup> S. Marka,<sup>1</sup> Z. Xu,<sup>1</sup> R. Godang,<sup>2</sup>  
 K. Kinoshita,<sup>2,\*</sup> I. C. Lai,<sup>2</sup> P. Pomianowski,<sup>2</sup> S. Schrenk,<sup>2</sup> G. Bonvicini,<sup>3</sup> D. Cinabro,<sup>3</sup>  
 R. Greene,<sup>3</sup> L. P. Perera,<sup>3</sup> G. J. Zhou,<sup>3</sup> S. Chan,<sup>4</sup> G. Eigen,<sup>4</sup> E. Lipeles,<sup>4</sup> J. S. Miller,<sup>4</sup>  
 M. Schmidtler,<sup>4</sup> A. Shapiro,<sup>4</sup> W. M. Sun,<sup>4</sup> J. Urheim,<sup>4</sup> A. J. Weinstein,<sup>4</sup> F. Würthwein,<sup>4</sup>  
 D. E. Jaffe,<sup>5</sup> G. Masek,<sup>5</sup> H. P. Paar,<sup>5</sup> E. M. Potter,<sup>5</sup> S. Prell,<sup>5</sup> V. Sharma,<sup>5</sup> D. M. Asner,<sup>6</sup>  
 J. Gronberg,<sup>6</sup> T. S. Hill,<sup>6</sup> D. J. Lange,<sup>6</sup> R. J. Morrison,<sup>6</sup> H. N. Nelson,<sup>6</sup> T. K. Nelson,<sup>6</sup>  
 D. Roberts,<sup>6</sup> B. H. Behrens,<sup>7</sup> W. T. Ford,<sup>7</sup> A. Gritsan,<sup>7</sup> H. Krieg,<sup>7</sup> J. Roy,<sup>7</sup> J. G. Smith,<sup>7</sup>  
 J. P. Alexander,<sup>8</sup> R. Baker,<sup>8</sup> C. Bebek,<sup>8</sup> B. E. Berger,<sup>8</sup> K. Berkelman,<sup>8</sup> V. Boisvert,<sup>8</sup>  
 D. G. Cassel,<sup>8</sup> D. S. Crowcroft,<sup>8</sup> M. Dickson,<sup>8</sup> S. von Dombrowski,<sup>8</sup> P. S. Drell,<sup>8</sup>  
 K. M. Ecklund,<sup>8</sup> R. Ehrlich,<sup>8</sup> A. D. Foland,<sup>8</sup> P. Gaidarev,<sup>8</sup> L. Gibbons,<sup>8</sup> B. Gittelman,<sup>8</sup>  
 S. W. Gray,<sup>8</sup> D. L. Hartill,<sup>8</sup> B. K. Heltsley,<sup>8</sup> P. I. Hopman,<sup>8</sup> J. Kandaswamy,<sup>8</sup>  
 D. L. Kreinick,<sup>8</sup> T. Lee,<sup>8</sup> Y. Liu,<sup>8</sup> N. B. Mistry,<sup>8</sup> C. R. Ng,<sup>8</sup> E. Nordberg,<sup>8</sup> M. Ogg,<sup>8,†</sup>  
 J. R. Patterson,<sup>8</sup> D. Peterson,<sup>8</sup> D. Riley,<sup>8</sup> A. Soffer,<sup>8</sup> B. Valant-Spaight,<sup>8</sup> A. Warburton,<sup>8</sup>  
 C. Ward,<sup>8</sup> M. Athanas,<sup>9</sup> P. Avery,<sup>9</sup> C. D. Jones,<sup>9</sup> M. Lohner,<sup>9</sup> C. Prescott,<sup>9</sup> A. I. Rubiera,<sup>9</sup>  
 J. Yelton,<sup>9</sup> J. Zheng,<sup>9</sup> G. Brandenburg,<sup>10</sup> R. A. Briere,<sup>10</sup> A. Ershov,<sup>10</sup> Y. S. Gao,<sup>10</sup>  
 D. Y.-J. Kim,<sup>10</sup> R. Wilson,<sup>10</sup> H. Yamamoto,<sup>10</sup> T. E. Browder,<sup>11</sup> Y. Li,<sup>11</sup> J. L. Rodriguez,<sup>11</sup>  
 S. K. Sahu,<sup>11</sup> T. Bergfeld,<sup>12</sup> B. I. Eisenstein,<sup>12</sup> J. Ernst,<sup>12</sup> G. E. Gladding,<sup>12</sup> G. D. Gollin,<sup>12</sup>  
 R. M. Hans,<sup>12</sup> E. Johnson,<sup>12</sup> I. Karliner,<sup>12</sup> M. A. Marsh,<sup>12</sup> M. Palmer,<sup>12</sup> M. Selen,<sup>12</sup>  
 J. J. Thaler,<sup>12</sup> K. W. Edwards,<sup>13</sup> A. Bellerive,<sup>14</sup> R. Janicek,<sup>14</sup> P. M. Patel,<sup>14</sup> A. J. Sadoff,<sup>15</sup>  
 R. Ammar,<sup>16</sup> P. Baringer,<sup>16</sup> A. Bean,<sup>16</sup> D. Besson,<sup>16</sup> D. Coppage,<sup>16</sup> C. Darling,<sup>16</sup>  
 R. Davis,<sup>16</sup> S. Kotov,<sup>16</sup> I. Kravchenko,<sup>16</sup> N. Kwak,<sup>16</sup> L. Zhou,<sup>16</sup> S. Anderson,<sup>17</sup>  
 Y. Kubota,<sup>17</sup> S. J. Lee,<sup>17</sup> R. Mahapatra,<sup>17</sup> J. J. O'Neill,<sup>17</sup> R. Poling,<sup>17</sup> T. Riehle,<sup>17</sup>  
 A. Smith,<sup>17</sup> M. S. Alam,<sup>18</sup> S. B. Athar,<sup>18</sup> Z. Ling,<sup>18</sup> A. H. Mahmood,<sup>18</sup> S. Timm,<sup>18</sup>  
 F. Wappler,<sup>18</sup> A. Anastassov,<sup>19</sup> J. E. Duboscq,<sup>19</sup> K. K. Gan,<sup>19</sup> T. Hart,<sup>19</sup> K. Honscheid,<sup>19</sup>  
 H. Kagan,<sup>19</sup> R. Kass,<sup>19</sup> J. Lee,<sup>19</sup> H. Schwarthoff,<sup>19</sup> A. Wolf,<sup>19</sup> M. M. Zoeller,<sup>19</sup>  
 S. J. Richichi,<sup>20</sup> H. Severini,<sup>20</sup> P. Skubic,<sup>20</sup> A. Undrus,<sup>20</sup> M. Bishai,<sup>21</sup> S. Chen,<sup>21</sup> J. Fast,<sup>21</sup>  
 J. W. Hinson,<sup>21</sup> N. Menon,<sup>21</sup> D. H. Miller,<sup>21</sup> E. I. Shibata,<sup>21</sup> I. P. J. Shipsey,<sup>21</sup> S. Glenn,<sup>22</sup>  
 Y. Kwon,<sup>22,‡</sup> A.L. Lyon,<sup>22</sup> S. Roberts,<sup>22</sup> E. H. Thorndike,<sup>22</sup> C. P. Jessop,<sup>23</sup> K. Lingel,<sup>23</sup>  
 H. Marsiske,<sup>23</sup> M. L. Perl,<sup>23</sup> V. Savinov,<sup>23</sup> D. Ugolini,<sup>23</sup> X. Zhou,<sup>23</sup> T. E. Coan,<sup>24</sup>  
 V. Fadeyev,<sup>24</sup> I. Korolkov,<sup>24</sup> Y. Maravin,<sup>24</sup> I. Narsky,<sup>24</sup> R. Stroynowski,<sup>24</sup> J. Ye,<sup>24</sup>  
 T. Wlodek,<sup>24</sup> M. Artuso,<sup>25</sup> E. Dambasuren,<sup>25</sup> S. Kopp,<sup>25</sup> G. C. Moneti,<sup>25</sup> R. Mountain,<sup>25</sup>  
 S. Schuh,<sup>25</sup> T. Skwarnicki,<sup>25</sup> S. Stone,<sup>25</sup> A. Titov,<sup>25</sup> G. Viehhauser,<sup>25</sup> and J.C. Wang<sup>25</sup>

<sup>1</sup>Vanderbilt University, Nashville, Tennessee 37235

<sup>2</sup>Virginia Polytechnic Institute and State University, Blacksburg, Virginia 24061

<sup>3</sup>Wayne State University, Detroit, Michigan 48202

<sup>4</sup>California Institute of Technology, Pasadena, California 91125

<sup>5</sup>University of California, San Diego, La Jolla, California 92093

---

\*Permanent address: University of Cincinnati, Cincinnati, OH 45221.

†Permanent address: University of Texas, Austin TX 78712.

‡Permanent address: Yonsei University, Seoul 120-749, Korea.

- <sup>6</sup>University of California, Santa Barbara, California 93106
- <sup>7</sup>University of Colorado, Boulder, Colorado 80309-0390
- <sup>8</sup>Cornell University, Ithaca, New York 14853
- <sup>9</sup>University of Florida, Gainesville, Florida 32611
- <sup>10</sup>Harvard University, Cambridge, Massachusetts 02138
- <sup>11</sup>University of Hawaii at Manoa, Honolulu, Hawaii 96822
- <sup>12</sup>University of Illinois, Urbana-Champaign, Illinois 61801
- <sup>13</sup>Carleton University, Ottawa, Ontario, Canada K1S 5B6  
and the Institute of Particle Physics, Canada
- <sup>14</sup>McGill University, Montréal, Québec, Canada H3A 2T8  
and the Institute of Particle Physics, Canada
- <sup>15</sup>Ithaca College, Ithaca, New York 14850
- <sup>16</sup>University of Kansas, Lawrence, Kansas 66045
- <sup>17</sup>University of Minnesota, Minneapolis, Minnesota 55455
- <sup>18</sup>State University of New York at Albany, Albany, New York 12222
- <sup>19</sup>Ohio State University, Columbus, Ohio 43210
- <sup>20</sup>University of Oklahoma, Norman, Oklahoma 73019
- <sup>21</sup>Purdue University, West Lafayette, Indiana 47907
- <sup>22</sup>University of Rochester, Rochester, New York 14627
- <sup>23</sup>Stanford Linear Accelerator Center, Stanford University, Stanford, California 94309
- <sup>24</sup>Southern Methodist University, Dallas, Texas 75275
- <sup>25</sup>Syracuse University, Syracuse, New York 13244

The semileptonic decays of the  $B$ -meson play important roles in heavy quark physics. They provide our best information on the CKM matrix elements  $V_{cb}$  and  $V_{ub}$  [1] and reveal the dynamics of heavy quark decay in their form factors. Heavy Quark Effective Theory (HQET) [2] provides a framework for calculating the form factors for  $b \rightarrow c\ell\nu$  decays and suggests a reliable method for extracting  $|V_{cb}|$  by predicting that QCD effects are small at the kinematic point where the final-state meson is at rest relative to the initial meson (zero recoil). Most studies of the form factors and  $|V_{cb}|$  [3] have used the  $B \rightarrow D^*\ell\nu$  decay because its differential branching fraction near the zero-recoil region is large and the QCD effects have been calculated to the highest accuracy [4]. There have been two recent studies of the mode  $B \rightarrow D\ell\nu$  [5] [6]. Here we present a new, more precise study of  $B \rightarrow D\ell\nu$  using a different analysis method.

We select  $B$  charm semileptonic decays including  $B \rightarrow D\ell\nu$ ,  $B \rightarrow D^*\ell\nu$ ,  $B \rightarrow D^{**}\ell\nu$ , and  $B \rightarrow D^{(*)}\pi\ell\nu$  decays by identifying events with a  $D$  ( $D^0$  or  $D^+$  and their charge conjugates) and a lepton. We then separate  $B \rightarrow D\ell\nu$  from the other semileptonic modes using the net energy and momentum of the particle or particles recoiling against the  $D - \ell$  pair. Information on the partial width and differential decay rate are obtained from the  $B^- \rightarrow D^0\ell^-\bar{\nu}$  and  $\bar{B}^0 \rightarrow D^+\ell^-\bar{\nu}$  yields, which we extract in bins of the HQET variable  $w = (M_B^2 + M_D^2 - q^2)/(2M_B M_D)$ , where  $q^2$  is the squared invariant mass of the virtual  $W$ .

The data used in this analysis were accumulated in the CLEO detector [7] at the Cornell Electron Storage Ring (CESR). The data consist of 3.3 million  $B\bar{B}$  events collected at the  $\Upsilon(4S)$  resonance. We also use  $1.6 \text{ fb}^{-1}$  of data collected 60 MeV below the  $\Upsilon(4S)$  resonance to study the background from the  $e^+e^- \rightarrow q\bar{q}$  continuum. The CLEO detector measures the trajectories of charged particles in a drift chamber system inside a 1.5T superconducting solenoid. The main drift chamber provides the specific ionization ( $dE/dx$ ) of charged particles and their time-of-flight (TOF) is provided by scintillation counters surrounding the drift chamber. A CsI electromagnetic calorimeter is used in electron identification. Muons register hits in counters embedded in steel surrounding the magnet.

In this analysis we select events having at least 5 charged tracks and, to suppress non- $B\bar{B}$  events, the ratio of Fox-Wolfram moments [8]  $H_2/H_0 < 0.45$ . We reconstruct  $D^0$  and  $D^+$  candidates in the decay modes  $D^0 \rightarrow K^-\pi^+$  and  $D^+ \rightarrow K^-\pi^+\pi^+$  respectively. We distinguish  $K$ 's from  $\pi$ 's based on a  $\chi^2$  probability ( $P_K$  and  $P_\pi$ ) that combines  $dE/dx$  and TOF. Each daughter track must satisfy  $P_i > 0.01$  and  $P_i/(P_K + P_\pi) > 0.3$ , where  $i$  is  $\pi$  or  $K$  as appropriate. The candidate mass must be within  $1.835 \text{ GeV} < m_{K\pi} < 1.893 \text{ GeV}$  for  $D^0$  and  $1.846 \text{ GeV} < m_{K\pi\pi} < 1.890 \text{ GeV}$  for  $D^+$  decays. To suppress  $D$ -mesons produced in  $e^+e^- \rightarrow c\bar{c}$  events, we require  $|\mathbf{p}_D| < 2.5 \text{ GeV}/c$ .

Electrons are identified using  $dE/dx$ , the shape of the shower in the CsI calorimeter, and  $E/p$ , the ratio of the candidate's energy deposit in the CsI to its momentum. Electrons are required to have momenta between  $0.8 \text{ GeV}/c$  and  $2.4 \text{ GeV}/c$ . Muons, selected within the same momentum window, must penetrate at least 5 interaction lengths of material. This requirement places an implicit lower bound on the muon momentum of about  $1.4 \text{ GeV}/c$ . We require that the lepton have the same charge as the  $K$  from the decay of the  $D$ -meson. Since the decaying  $B$ -meson is nearly at rest, the  $D$ -meson and the lepton are in opposite hemispheres for more than 90% of  $B \rightarrow D\ell\nu$  decays; we demand that this be so.

For events satisfying these criteria, we compute  $\cos\theta_{B-D\ell}$ , the cosine of the angle between the  $D\ell$  momentum  $\mathbf{p}_{D\ell} = \mathbf{p}_D + \mathbf{p}_\ell$  and the  $B$  momentum  $\mathbf{p}_B$ , assuming that the decay is

TABLE I. Yields and Backgrounds. Uncertainties are statistical only.

|                                 | $D^0\ell$       | $D^+\ell$       |
|---------------------------------|-----------------|-----------------|
| Total Yield                     | $12595 \pm 112$ | $18087 \pm 134$ |
| Random $K\pi(\pi)$ Combinations | $5083 \pm 50$   | $13502 \pm 70$  |
| Uncorrelated                    | $948 \pm 63$    | $761 \pm 75$    |
| Continuum                       | $452 \pm 84$    | $432 \pm 104$   |
| Correlated                      | $119 \pm 16$    | $119 \pm 23$    |
| Fake Lepton                     | $71 \pm 19$     | $26 \pm 25$     |
| Background-subtracted Yield     | $5922 \pm 163$  | $3247 \pm 201$  |

$B \rightarrow D\ell\nu$  and that the only missing  $B$  particle is the massless neutrino; that is

$$\cos\theta_{B-D\ell} = \frac{2E_B E_{D\ell} - M_B^2 - M_{D\ell}^2}{2|\mathbf{p}_B||\mathbf{p}_{D\ell}|}. \quad (1)$$

This quantity lies between  $-1.0$  and  $1.0$  for  $B \rightarrow D\ell\nu$  decays. When final-state particles are missing in addition to the  $\nu$ , as is the case for the other  $B$  semileptonic decay modes,  $\cos\theta_{B-D\ell}$  decreases. We use the distribution of  $\cos\theta_{B-D\ell}$  to separate  $B \rightarrow D\ell\nu$  events from the other  $B$  semileptonic decay modes after subtracting backgrounds.

The backgrounds come from several sources: random  $K\pi(\pi)$  combinations,  $D$ -mesons matched with a lepton from the other  $B$  decay (uncorrelated),  $D$ -mesons combined with a lepton that is a granddaughter of the same  $B$  (correlated), hadrons misidentified as leptons (fake lepton), and  $e^+e^- \rightarrow q\bar{q}$  events.

Events in the mass regions above and below the  $D$  peak (sideband) are utilized to estimate the random combination contribution. A study using Monte Carlo-simulated  $B$  decays shows that this method subtracts the right amount of background within small uncertainties and that the  $\cos\theta_{B-D\ell}$  distribution of the events in the sidebands reproduces that of the background events in the signal region.

In uncorrelated background events, the angular distribution between the  $D$  and  $\ell$  is nearly uniform because they arise from different  $B$ -mesons, both nearly at rest. We take advantage of this uniformity: for each event in which the  $D$  and  $\ell$  are in the same hemisphere we reverse the lepton's direction and compute  $\cos\theta_{B-D\ell}$ , thereby constructing this distribution for the opposite-hemisphere background events.

The  $e^+e^- \rightarrow q\bar{q}$  continuum background is measured using events collected off resonance. The correlated background, which is small, arises from modes such as  $B \rightarrow D_s D$  followed by  $D_s \rightarrow X\ell\nu$  and  $B \rightarrow DX\tau\nu$  followed by  $\tau \rightarrow \ell\nu\bar{\nu}$ . We estimate these contributions using a Monte Carlo simulation. Fake lepton background is estimated by repeating the analysis using hadrons in place of leptons and then scaling the yield by the momentum-dependent electron and muon misidentification probabilities. Table I summarizes the data yield and backgrounds.

After subtracting the backgrounds, we are left with  $B \rightarrow D^0 X\ell\nu$  and  $B \rightarrow D^+ X\ell\nu$  decays, where  $X$  stands for zero or more pions or photons. We divide each of these samples into ten equal bins of  $\tilde{w}$  in the range  $1.0 \leq \tilde{w} < 1.6$ , where  $\tilde{w}$  is the reconstructed value of  $w$ , and is smeared by the detector resolution and motion of the  $B$ . In each  $\tilde{w}$  bin we

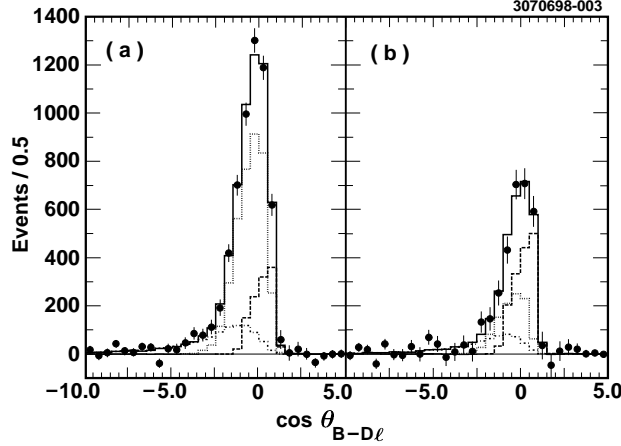


FIG. 1. The  $\cos\theta_{B-D\ell}$  distribution for (a)  $B \rightarrow D^0 X \ell \nu$  and (b)  $B \rightarrow D^+ X \ell \nu$ . The data (solid circles) are overlaid with simulated  $B \rightarrow D \ell \nu$  decays (dashed histogram),  $B \rightarrow D^* \ell \nu$  decays (dotted histogram),  $B \rightarrow D^{**} \ell \nu + D^{(*)} \pi \ell \nu$  decays (dash-dotted histogram), and their total (solid histogram). The normalizations of the simulated samples are provided by the fit.

fit the  $\cos\theta_{B-D\ell}$  distributions of the  $B \rightarrow D^0 X \ell \nu$  and  $B \rightarrow D^+ X \ell \nu$  samples for the yields of  $D \ell \nu$ ,  $D^* \ell \nu$  and the sum of  $D^{**} \ell \nu$  and  $D^{(*)} \pi \ell \nu$ , using Monte Carlo-simulated  $\cos\theta_{B-D\ell}$  distributions for each of these modes. In the simulation, we model  $B \rightarrow D \ell \nu$  decays using ISGW2 [9] and  $B \rightarrow D^* \ell \nu$  decays using the form factors measured by CLEO [10]. We model the  $D^{**}$  mesons with radial and angular excitations using ISGW2 and non-resonant  $D^{(*)} \pi$  states using the results of Goity and Roberts [11]. The detector simulation is based on GEANT [12]. In our fits, we apply the isospin symmetry constraint that the ratio of  $B \rightarrow D^* \ell \nu$  to  $B \rightarrow D \ell \nu$  decay rates should be the same for charged and neutral  $B$ -meson decays. Figure 1 shows the result of a fit over all  $\tilde{w}$ . The sum of the  $B^- \rightarrow D^0 \ell^- \bar{\nu}$  and  $\bar{B}^0 \rightarrow D^+ \ell^- \bar{\nu}$  yields as a function of  $\tilde{w}$  are displayed in Figure 2. These  $\tilde{w}$  distributions are the basis of our studies of the  $B^- \rightarrow D^0 \ell^- \bar{\nu}$  and  $\bar{B}^0 \rightarrow D^+ \ell^- \bar{\nu}$  form factor and decay rate.

The differential decay width of  $B \rightarrow D \ell \nu$  is given by [4]

$$\frac{d\Gamma}{dw} = \frac{G_F^2 |V_{cb}|^2}{48\pi^3} (m_B + m_D)^2 m_D^3 (w^2 - 1)^{3/2} F_D(w)^2, \quad (2)$$

where  $G_F$  is the weak coupling constant,  $m_D$  is the mass of the  $D^0$  or  $D^+$  and  $F_D(w)$  is the form factor. We fit the  $B^- \rightarrow D^0 \ell^- \bar{\nu}$  and  $\bar{B}^0 \rightarrow D^+ \ell^- \bar{\nu}$  yields in the intervals with  $\tilde{w} > 1.12$  to extract information on  $|V_{cb}|$  and the form factor. The two bins with  $\tilde{w} < 1.12$  are excluded because they suffer from small rates due to the  $(w^2 - 1)^{3/2}$  suppression and large backgrounds. In our fit, the  $\chi^2$  function for  $B^- \rightarrow D^0 \ell^- \bar{\nu}$  is expressed as

$$\chi_{D^0 \ell^- \bar{\nu}}^2 = \sum_{i=3}^{10} \frac{[N_i^{obs} - \sum_{j=1}^{10} \epsilon_{ij} N_j]^2}{\sigma_{N_i^{obs}}^2 + \sum_{j=1}^{10} \sigma_{\epsilon_{ij}}^2 N_j^2}, \quad (3)$$

where  $N_i^{obs}$  is the yield in the  $i$ th  $\tilde{w}$  bin and

$$N_j = 2f_{+-} N_{\Upsilon(4S)} \mathcal{B}_{K\pi} \tau_{B^-} \int_{w_j} dw d\Gamma/dw \quad (4)$$

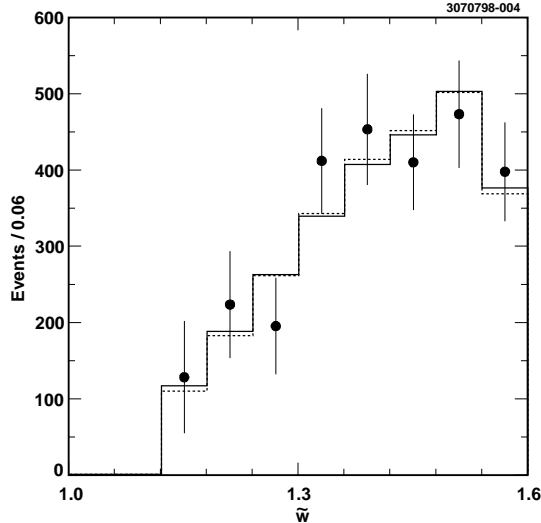


FIG. 2. The sum of  $B^- \rightarrow D^0 \ell^- \bar{\nu}$  and  $\bar{B}^0 \rightarrow D^+ \ell^- \bar{\nu}$  yields as a function of  $\tilde{w}$ , for the data (solid circles) and using the best fit linear form factor (dashed histogram) or dispersion relation inspired form factor of Boyd *et al.* (solid histogram).

is the number of decays in the  $j$ th  $w$  bin implied by the fit parameters. Here  $\tau_{B^-}$  is the  $B^-$  lifetime [13],  $\mathcal{B}_{K\pi}$  is the  $D^0 \rightarrow K^- \pi^+$  branching fraction [14],  $N_{\Upsilon(4S)}$  is the number of  $\Upsilon(4S)$  events in the sample, and  $f_{+-}$  is the  $\Upsilon(4S) \rightarrow B^+ B^-$  branching fraction. An efficiency matrix,  $\epsilon_{ij}$ , accounts for reconstruction efficiency and for the smearing of  $\tilde{w}$ . The fraction of decays in each  $w$  bin that are reconstructed ranges between 17% and 21% and the average  $\tilde{w}$  resolution is 0.026, about one-half the bin width. The small Monte Carlo statistical uncertainty in the efficiency matrix is represented by  $\sigma_{\epsilon_{ij}}^2$ . We form  $\chi_{D^+ \ell^- \bar{\nu}}^2$  analogously. In the fits, we minimize  $\chi^2 = \chi_{D^+ \ell^- \bar{\nu}}^2 + \chi_{D^0 \ell^- \bar{\nu}}^2$ , varying  $|V_{cb}|F_D(1)$ , the coefficients in the parametrization of  $F_D(w)/F_D(1)$ , and  $f_{+-}$ . We assume that the form factor parameters are common to  $D^0 \ell^- \bar{\nu}$  and  $D^+ \ell^- \bar{\nu}$  decays and that  $B^+ B^-$  and  $B^0 \bar{B}^0$  together saturate  $\Upsilon(4S)$  decays.

We investigate several parametrizations of the form factor. Results for all of these are summarized in Table II. In all fits we find  $f_{+-} = 0.49 \pm 0.04$ , consistent with previous measurements [15], and similar correlation coefficients. We first consider the common expansion  $F_D(w)/F_D(1) = 1 - \rho_D^2(w-1) + c_D(w-1)^2$ . When  $c_D$  is constrained to be zero, we find  $\rho_D^2 = 0.76 \pm 0.16$  and  $|V_{cb}|F_D(1) = 0.0405 \pm 0.0045$  with the correlation coefficients  $\rho(|V_{cb}|F_D(1), \rho_D^2) = 0.95$ ,  $\rho(|V_{cb}|F_D(1), f_{+-}) = 0.12$  and  $\rho(f_{+-}, \rho_D^2) = 0.03$ . The  $\chi^2$  is 8.8 for 13 degrees of freedom. When the  $D^0 \ell^- \bar{\nu}$  and  $D^+ \ell^- \bar{\nu}$  samples are fit separately, they give consistent results for all parameters. This form factor is superimposed on the data in Figure 2. When  $c_D$  is allowed to vary, we find that it is consistent with zero within large errors; that is, our data allow substantial curvature but do not require it. In this fit,  $\rho_D^2$  and  $c_D$  are completely correlated because our data are most precise at large values of  $w$ .

Dispersion relations constrain the form factor. Boyd *et al.* [16] expand the form factor in the variable  $z = (\sqrt{w+1} - \sqrt{2N})/(\sqrt{w+1} + \sqrt{2N})$ , where  $N \approx 1.1$ . Because  $z$  is small, this expansion converges more rapidly than one in  $w-1$ . Fitting for the linear coefficient  $a_1$  with  $N = 1.108$ , we find  $a_1 = -0.043 \pm 0.027$ . Expanding this form factor in powers of  $w-1$  yields  $\rho_D^2 = 1.30 \pm 0.27$  and  $c_D = 1.21 \pm 0.31$  plus higher order terms. Caprini *et al.* [17] have

TABLE II. Summary of the  $B \rightarrow D\ell\nu$  form factor fits. In addition to the quoted statistical uncertainties, there are fractional systematic uncertainties of 12% in  $\rho_D^2$  and  $c_D$  and 8% in  $|V_{cb}|F_D(1)$ .

| Form factor                        | $\rho_D^2$             | $c_D$                  | $10^2 V_{cb} F_D(1)$   | $\chi^2/dof$ |
|------------------------------------|------------------------|------------------------|------------------------|--------------|
| Linear                             | $0.76 \pm 0.16$        | –                      | $4.05 \pm 0.45$        | 8.8/13       |
| Parabolic                          | $0.77^{+1.18}_{-2.83}$ | $0.01^{+1.70}_{-3.96}$ | $4.05^{+1.51}_{-1.63}$ | 8.8/12       |
| Boyd <i>et al.</i> * <sup>†</sup>  | $1.30 \pm 0.27$        | $1.21 \pm 0.31$        | $4.48 \pm 0.61$        | 8.9/13       |
| Caprini <i>et al.</i> <sup>†</sup> | $1.27 \pm 0.25$        | $1.18 \pm 0.26$        | $4.44 \pm 0.58$        | 8.9/13       |

\* We find  $a_1 = -0.043 \pm 0.027$  for  $N = 1.108$ .

<sup>†</sup> This form factor also has terms of order  $(w - 1)^3$  and higher.

also used dispersion relations to constrain the form factors. Their parametrization leads to similar results.

To obtain the  $B \rightarrow D\ell\nu$  decay rate, we use the form factor parameters provided by the fits and integrate  $d\Gamma/dw$  over  $w$ . The form factor of Boyd *et al.* [16] gives  $\Gamma = (14.1 \pm 1.0) \text{ ns}^{-1}$ . The other parametrizations give the same result within 1%.

The systematic uncertainties are given in Table III. The uncertainties in the  $B$ -meson momentum and mass dominate because they respectively affect the width and mean of the  $\cos\theta_{B-D\ell}$  distributions and therefore the  $D^0\ell^-\bar{\nu}$  and  $D^+\ell^-\bar{\nu}$  yields extracted in each  $\tilde{w}$  bin. We have tuned our simulation to reproduce the  $B$  momentum distribution observed in fully reconstructed  $B$  decays; however, there is a 6 MeV uncertainty in the mean and this leads to fractional systematic uncertainties of 5% for  $\rho_D^2$ , 4% for  $|V_{cb}|F_D(1)$  and 3% for  $\Gamma$ . The 1.8 MeV [18] uncertainty in the  $B$  mass generates uncertainties of 7% for  $\rho_D^2$ , 4% for  $|V_{cb}|F_D(1)$  and 3% for  $\Gamma$ .

The other large systematic error arises from uncertainty in the  $\cos\theta_{B-D\ell}$  distribution of the combined  $B \rightarrow D^{**}\ell\nu$  and  $B \rightarrow D^{(*)}\pi\ell\nu$  backgrounds. This distribution depends mainly on the number of final-state pions that are not reconstructed. We therefore separate it into two components: one in which the final-state  $D$  is accompanied by one  $\pi$  and the other in which it is accompanied by two. We vary their relative proportions from 1:4 to 2:3 [19] to evaluate the systematic uncertainty.

The  $B \rightarrow D^*\ell\nu$  form factors affect the distribution of these decays in  $\cos\theta_{B-D\ell}$  and therefore influence the extracted  $B \rightarrow D\ell\nu$  yield. We vary the form factors within the uncertainties of the CLEO measurement [10], taking into account the correlations among the form factor parameters ( $R_1, R_2$  and  $\rho^2$ ).

The slope of the  $B \rightarrow D\ell\nu$  form factor is varied in our fit so its uncertainty is included in the statistical error in the decay width. Using a linear form factor to extract the width rather than the dispersion-relation-inspired form factor changes the width by 0.8%. The form factor can also affect the  $\cos\theta_{B-D\ell}$  distribution used to extract the  $D^0\ell^-\bar{\nu}$  and  $D^+\ell^-\bar{\nu}$  yields in each  $\tilde{w}$  bin and the efficiency matrix. Each of these effects is less than 1%.

Our final result is

$$\Gamma(B \rightarrow D\ell\nu) = (14.1 \pm 1.0 \pm 1.2) \text{ ns}^{-1}. \quad (5)$$

Multiplying this by the measured  $B$ -meson lifetimes gives the branching fractions



TABLE III. The fractional systematic uncertainties.

| Source                     | $\rho_D^2$ | $ V_{cb} F_D(1)$ | $\Gamma(B \rightarrow D\ell\nu)$ |
|----------------------------|------------|------------------|----------------------------------|
| Track-finding              | –          | 0.02             | 0.035                            |
| Lepton ID                  | –          | 0.01             | 0.020                            |
| $K$ and $\pi$ ID           | 0.02       | 0.01             | 0.022                            |
| Backgrounds                | 0.06       | 0.04             | 0.018                            |
| $ \mathbf{p}_B $ and $M_B$ | 0.08       | 0.05             | 0.042                            |
| Luminosity                 | –          | 0.01             | 0.018                            |
| $D\ell\nu$ form factor     | 0.01       | 0.01             | 0.010                            |
| $D^*\ell\nu$ form factors  | 0.01       | 0.01             | 0.005                            |
| $D^{**}\ell\nu$ model      | 0.04       | 0.03             | 0.026                            |
| $D$ branching fractions    | –          | 0.02             | 0.036                            |
| $\tau_B$                   | –          | 0.02             | 0.026                            |
| Total                      | 0.11       | 0.08             | 0.085                            |

$$\mathcal{B}(B^- \rightarrow D^0 \ell^- \bar{\nu}) = (2.32 \pm 0.17 \pm 0.20)\% \quad \text{and} \quad (6)$$

$$\mathcal{B}(\bar{B}^0 \rightarrow D^+ \ell^- \bar{\nu}) = (2.20 \pm 0.16 \pm 0.19)\%, \quad (7)$$

where the first errors are statistical and the second are systematic. Since we derive both branching fractions from the decay width, their errors are completely correlated. This result is consistent with previous measurements but is more precise. Combining it with the previous CLEO measurement [5], taking into account statistical and systematic correlations, gives

$$\Gamma(B \rightarrow D\ell\nu) = (13.4 \pm 0.8 \pm 1.2) \text{ ns}^{-1}, \quad (8)$$

$$\mathcal{B}(B^- \rightarrow D^0 \ell^- \bar{\nu}) = (2.21 \pm 0.13 \pm 0.19)\%, \quad \text{and} \quad (9)$$

$$\mathcal{B}(\bar{B}^0 \rightarrow D^+ \ell^- \bar{\nu}) = (2.09 \pm 0.13 \pm 0.18)\%, \quad (10)$$

where the errors in the partial width and branching fractions are completely correlated.

Our studies of the form factor give  $\rho_D^2 = 0.76 \pm 0.16 \pm 0.08$  (linear fit) and  $\rho_D^2 = 1.30 \pm 0.27 \pm 0.14$  and  $c_D = 1.21 \pm 0.31 \pm 0.15$  plus higher order terms (dispersion relations). The latter gives

$$|V_{cb}|F_D(1) = (4.48 \pm 0.61 \pm 0.37) \times 10^{-2}. \quad (11)$$

Various authors have found  $F_D(1) = 0.98 \pm 0.07$  [20] and  $F_D(1) = 1.03 \pm 0.07$  [9], and a recent lattice calculation finds the preliminary value  $F_D(1) = 1.069 \pm 0.029$  [21]. Using  $F_D(1) = 1.0$ , we find  $|V_{cb}| = 0.045 \pm 0.006 \pm 0.004 \pm 0.005$ , where the last uncertainty covers all of these values of  $F_D(1)$ . This value of  $|V_{cb}|$  is consistent with that from  $B \rightarrow D^*\ell\nu$  decays, though its uncertainty is larger. Using the linear form factor, as has been done in most previous studies of  $B \rightarrow D^*\ell\nu$ , gives a value of  $|V_{cb}|$  that is about 10% smaller than this. While the curvature of the form factor is likely to have a smaller effect on the  $|V_{cb}|$  extracted from  $B \rightarrow D^*\ell\nu$  decays, its effect could nevertheless be important.

We thank C.Glenn Boyd and Matthias Neubert for useful discussions. We gratefully acknowledge the effort of the CESR staff in providing us with excellent luminosity and running conditions. This work was supported by the National Science Foundation, the U.S. Department of Energy, Research Corporation, the Natural Sciences and Engineering Research

Council of Canada, the A.P. Sloan Foundation, the Swiss National Science Foundation, and the Alexander von Humboldt Stiftung.

## REFERENCES

- [1] N. Cabibbo, Phys. Rev. Lett. **10**, 531 (1963); M. Kobayashi and T. Maskawa, Prog. Theor. Phys. **49**, 652 (1973).
- [2] N. Isgur and M.B. Wise, Phys. Lett. B **232**, 113 (1989); N. Isgur and M.B. Wise, Phys. Lett. B **237**, 527 (1990); M. Neubert, Phys. Lett. B **264**, 455 (1991); M. Neubert, Phys. Rep. **245**, 259 (1994).
- [3] P. Drell, preprint CLNS 97/1521, hep-ex/9711020, Proceedings of the 18th International Symposium on Lepton-Photon Interactions, Hamburg (1997).
- [4] M. Neubert, Phys. Lett. **B264**, 455 (1991).
- [5] M. Athanas *et al.*, Phys. Rev. Lett. **79**, 2208 (1997).
- [6] D. Buskulic *et al.*, Phys. Lett. **B395**, 373 (1997).
- [7] Y. Kubota *et al.*, Nucl. Instrum. Methods Phys. Res., Sect. A **320**, 66 (1992).
- [8] G. Fox and S. Wolfram, Phys. Rev. Lett. **41**, 1581 (1978).
- [9] D. Scora and N. Isgur, Phys. Rev. D **52**, 2783 (1995); N. Isgur *et al.*, Phys. Rev. D **39**, 799 (1989).
- [10] J.E. Duboscq *et al.*, Phys. Rev. Lett. **76**, 3898 (1996).
- [11] J.L. Goity and W. Roberts, Phys. Rev. D **51**, 3459 (1995).
- [12] R. Brun *et al.*, GEANT 3.15, CERN DD/EE/84-1.
- [13] We use  $\tau_{B^-} = (1.65 \pm 0.04)$  ps and  $\tau_{\bar{B}^0} = (1.56 \pm 0.04)$  ps; Particle Data Group, Eur. Phys. J. C **3**, 1 (1998).
- [14] We use  $\mathcal{B}(D \rightarrow K\pi) = 0.0385 \pm 0.0009$  and  $\mathcal{B}(D \rightarrow K\pi\pi) = 0.090 \pm 0.006$ ; Ibid.
- [15] C.S. Jessop *et al.*, Phys. Rev. Lett. **79**, 4533 (1997).
- [16] C.G. Boyd, B. Grinstein and R.F. Lebed, Phys. Rev. D **56**, 6895(1997).
- [17] I. Caprini, L. Lellouch and M. Neubert, CERN-TH/97-91, hep-ph/9712417; submitted to Nucl. Phys. B.
- [18] Particle Data Group, Eur. Phys. J. C **3**, 1 (1998).
- [19] D. Buskulic *et al.*, ALEPH Collaboration, Z. Phys. **C73**, 601 (1997).
- [20] I. Caprini and M. Neubert, Phys. Lett. B **380**, 376 (1996).
- [21] S. Hashimoto, Sixteenth International Symposium on Lattice Field Theory (Lattice '98), Boulder, Colorado, July 13 - 18, 1998.